Mechanism of interfacial magnetoelectric coupling in composite multiferroics

C.-L. Jia,[1,2,*] T.-L. Wei,[1] C.-J. Jiang,[1] D.-S. Xue,[1] A. Sukhov,[2] and J. Berakdar[2,†]

[1]*Key Laboratory for Magnetism and Magnetic Materials of MOE, Lanzhou University, Lanzhou 730000, China*

[2]*Institut für Physik, Martin-Luther Universität, Halle-Wittenberg, 06099 Halle (Saale), Germany*

(Received 20 February 2014; revised manuscript received 8 August 2014; published 27 August 2014)

We work out theoretically a mechanism for magnetoelectric (ME) coupling driven by a buildup of an interfacial spiral spin density in ferromagnet (FM)/ferroelectric (FE) composites. We infer an intrinsic linear ME coupling that is most pronounced in the vicinity of the FM/FE interface acting within the spin-diffusion length λ_m of the order of nanometers. Our study delivers a strong coupling strength for Co(40 nm)/$BaTiO_3$ that is in line with experiments. We identify a region of magnetic noncollinearity coupled to dielectric polarization that extends over λ_m around the interface, functionalizing the interface for electric control of magnetotransport and surface magnetic anisotropy.

DOI: 10.1103/PhysRevB.90.054423 PACS number(s): 75.85.+t, 71.15.Mb, 75.70.Cn, 77.80.−e

I. INTRODUCTION

A multitude of fascinating emergent phenomena occur at the interface of heterestructures, an observation that is attracting intense research so as to clarify the underlying physics and the potential for novel technological applications (e.g., [1–4]). For instance, in the quest for multifunctional low-energy consumption devices, efforts are devoted to making it possible to steering magnetism with external electric fields via interfacing ferromagnetic (FM) and ferroelectric (FE) materials. This may result in interfacial magnetoelectric (ME) coupling. Indeed, along this line a series of findings have been reported, such as voltage-induced magnetic anisotropy in thin FM metal films [5–8] and synthesized functional multiferroic FM/FE heterostructures [9–13]. The route to understanding the direct ME coupling has been so far mostly via *first-principles* calculations [14–21] which have yielded a wealth of essential information on the complex interplay of spin-dependent interfacial charge transfer, chemical bonding, and electrostatic screening [22,23]. On the other hand, the well-established theory of magnetically driven ferroelectricity in single-phase multiferroics has proven very fruitful [24–29]. A counterpart of this theory is however still missing for interfacial ME effects, in particular to uncover when, where, and which ME coupling mechanism is active in FM/FE composites. The present study is a contribution to fill this gap. This endeavor is highly desirable, for tailoring FM/FE composites holds the promise of enhancing the ME coupling strength which is notoriously small in bulk matter.

We further aim at clarifying the puzzle of the large extension (compared to the screening length) of surface ME coupling [10,11,30,31], which we think is important for understanding and controlling ME properties of FM interfaces.

Here we demonstrate that spin-current-based multiferroicity is a key element for interface ME coupling: Interfacing FM with FE triggers in the FM low-energy (coherent magnonic) excitations near the interface, which builds up a spatially inhomogeneous, spin-current-carrying surface magnetic order within the spin-diffusion length (on the order of nanometers). Two contributions are identified: (1) Quasistatic screening spins, which follow adiabatically the direction of local magnetic moments, yield a linear ME effect. (2) Deviations from adiabaticity give rise to an exponential spiral spin density which goes along with an emergent electric response associated with the intrinsic spin current of the spiral [25,28]. The back action on the FE interface may result in structural rearrangement in the FE.

II. SURFACE SPIRAL SPIN DENSITY

Zhang [32] considered charge screening effects at a FM/dielectric interface within the linearized Thomas-Fermi model and estimated the surface screening length to be less than 2 Å for typical FM metals such as Ni, Co, or Fe. Experimentally [10,11,30,31], however, the region in which the spin order is affected extends far into the FM layer reaching nanometers near the FM/FE interface. We note, for Co/P VinyliDene Fluoride-TriFluoroEthylene (VDF-TrFE) (cf. Ref. [10]), the ME effect is expected to be due to screening because strain effects and atomic rearrangements at the interface are unimportant due to the substantial mismatch between the Co/P(VDF-TrFE) stiffness coefficients and weak interfacial coupling. Considering the usually weak ME coupling, the steady-state charge accumulation within a few angstroms (which entails particle-hole processes) in FM is energetically higher that the lower energy spin (waves) excitations [33] that should be of a major relevance and hence will be analyzed here.

To this end and to capture in general the induced spin imbalance, we employ the spin-density operator in standard second-quantized notation $\hat{\mathbf{s}} = \sum_{\sigma\sigma'} \psi^\dagger_\sigma(\mathbf{r})\hat{\boldsymbol{\sigma}}_{\sigma\sigma'}\psi_{\sigma'}(\mathbf{r})$ using creation $\psi^\dagger_\sigma$ and annihilation ψ_σ operators for an electron at point $\mathbf{r}$ and spin $\frac{\hbar}{2}\boldsymbol{\sigma}$, with $\{\psi_\sigma(\mathbf{r}), \psi^\dagger_{\sigma'}(\mathbf{r}')\} = \delta(\mathbf{r}-\mathbf{r}')\delta_{\sigma\sigma'}$. In a mean-field formulation, $\hat{\mathbf{s}}$ is exchange coupled to the localized spins $\mathbf{S}$ which are treated as classical variables since quantum fluctuations of $\mathbf{S}$ are suppressed by the strong FM exchange interaction ($J_{ex} \sim 0.1$ eV/atom [1]; for the justifications and details of mapping the itinerant system to an effective Heisenberg-type model we refer to [34]). The Hamiltonian for the independent itinerant electrons (with effective mass m) reads

$$H = \frac{\hbar^2}{2m}\sum_\sigma \int d\mathbf{r}\nabla\psi^\dagger_\sigma(\mathbf{r})\cdot\nabla\psi_\sigma(\mathbf{r}) + \int d\mathbf{r}[V(\mathbf{r})\hat{n}(\mathbf{r}) + H_{sd}]. \quad (1)$$

*cljia@lzu.edu.cn

†jamal.berakdar@physik.uni-halle.de

The first term is the kinetic energy; the second term is the interface potential with the electrostatic potential $V(r)\hat{n}(r)$; $\hat{n}(r) = (-e)\sum_\sigma \psi^\dagger_\sigma(r)\psi_\sigma(r)$ is the charge-density operator. The local s-d exchange interaction is [35] $H_{sd} = J_{ex}\hat{\mathbf{s}}\cdot\mathbf{e}_{M_\parallel}$ with $\mathbf{e}_{M_\parallel} = \mathbf{M}/M_s$ and the classically treated effective magnetization $\mathbf{M} = -\frac{g\mu_B}{a^3}\mathbf{S}$, where μ_B, g, and a are the Bohr magneton, g factor, and lattice constant, respectively. M_s is the intrinsic saturation magnetization. For ordered systems $\mathbf{M}$ is spatially periodically distributed. The dynamics of the spin density is governed by the Heisenberg equation of motion $\frac{d\hat{\mathbf{s}}}{dt} = \frac{1}{i\hbar}[\hat{\mathbf{s}}, H]$. Adopting a semiclassical approach and taking the average $\langle\cdots\rangle$ over all electron states, we obtain the Bloch equation for the spin density $\mathbf{s} = \langle\hat{\mathbf{s}}\rangle$ [36],

$$\frac{d\mathbf{s}}{dt} + \nabla\cdot\mathcal{J} = -\frac{1}{\tau_{ex}}\mathbf{s}\times\mathbf{e}_{M_\parallel} - \frac{\mathbf{s}}{\tau_{sf}}. \tag{2}$$

$\mathcal{J} = \frac{\hbar}{2m}\langle\Im[\psi^\dagger\hat{\boldsymbol{\sigma}}\otimes\nabla\psi]\rangle$ is the spin current density including the nonequilibrium surface electronic charge buildup and $\tau_{ex} = \hbar/(2J_{ex})$. The spin-flip relaxation time τ_{sf} is due to scattering with impurities, electrons, and phonons. As J_{ex} is much larger than magnon excitation energies we can employ an adiabatic procedure in which the induced spin density consists of two parts,

$$\mathbf{s}(\mathbf{r},t) = \mathbf{s}_\parallel(\mathbf{r},t) + \mathbf{s}_\perp(\mathbf{r},t). \tag{3}$$

$\mathbf{s}_\parallel$ is the spin density whose direction follows in an adiabatic sense the magnetization at an instantaneous time t, i.e., $\mathbf{s}_\parallel = s_\parallel\mathbf{e}_{M_\parallel}$. The transverse deviation from $\mathbf{M}$ is given by $\mathbf{s}_\perp$.

In the absence of a charge current across the FM/(insulating) FE heterostructure, the spin current is related only to the nonequilibrium spin density $\mathbf{s}$ normal to the interface (hereafter referred to as the $\mathbf{e}_z$ direction;the z axis has its origin at the interface) via

$$\mathcal{J}_\parallel = -D_0\nabla_z\mathbf{s}_\parallel \quad\text{and}\quad \mathcal{J}_\perp = -D_0\nabla_z\mathbf{s}_\perp, \tag{4}$$

where D_0 is the diffusion constant. From Eqs. (2)–(4) we obtain the stationary form for the nontrivial spin-density dynamics in the linear response limit,

$$D_0\nabla_z^2\mathbf{s}_\parallel = \frac{\mathbf{s}_\parallel}{\tau_{sf}}, \tag{5}$$

$$D_0\nabla_z^2\mathbf{s}_\perp = \frac{1}{\tau_{ex}}\mathbf{s}_\perp\times\mathbf{e}_{M_\parallel} + \frac{\mathbf{s}_\perp}{\tau_{sf}}. \tag{6}$$

For long-range magnetic ordering in typical FM metals and alloys at room temperature, $\tau_{ex}/\tau_{sf} \approx 10^{-2}$ [37], the interface spin density $\mathbf{s} = [s_\perp^x, s_\perp^y, s_\parallel]$ in the rotating frame around $\mathbf{M}$ is given by

$$s_\parallel = C_\parallel e^{-z/\lambda_m}, \tag{7}$$

$$s_\perp^x + is_\perp^y \approx C_\perp e^{-(1-i)\mathbf{Q}_m\cdot\mathbf{r}+i\theta_0}. \tag{8}$$

θ_0 is the initial phase. We find thus a local spiral spin density with the spin-wave vector $\mathbf{Q}_m = \frac{1}{\sqrt{2D_0\tau_{ex}}}[0,0,1]$ normal to the interface, regardless of the direction of $\mathbf{M}$ (see Fig. 1). $\lambda_m = \sqrt{D_0\tau_{sf}}$ is the effective spin-diffusion length at the surface. In general λ_m differs from the bulk value (8.5 ± 1.5 nm in Fe and 38 ± 12 nm in Co [37]); however, in the presence of exchange interaction with long-range magnetic ordering, the

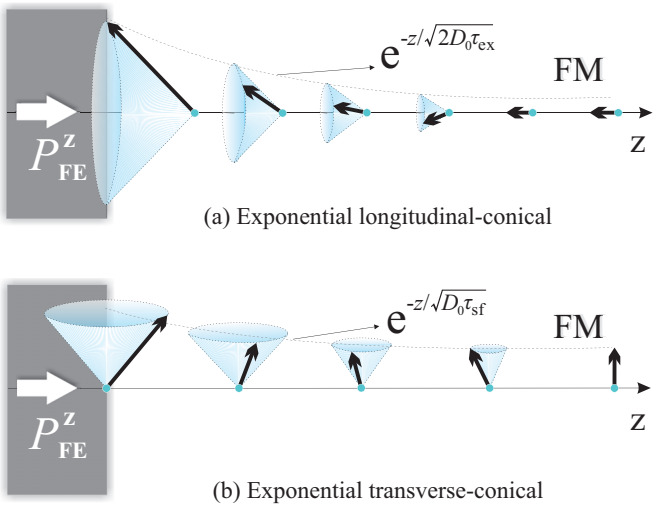

FIG. 1. (Color online) Exponential spiral spin density $\tilde{\mathbf{M}}(\mathbf{r}) = \mathbf{M}(\mathbf{r}) + \mathbf{s}(\mathbf{r})$ in a FM near a FM/FE interface ($z = 0$). The intrinsic FM magnetization $\mathbf{M}(\mathbf{r})$ (i.e., for $z \gg 1$) is (a) normal to the interface $\mathbf{M} \parallel \mathbf{e}_z$ or (b) in the interface plane. The induced surface spin density $\mathbf{s}(\mathbf{r})$, consisting of the adiabatic term ($\mathbf{s}_\parallel$) along $\mathbf{M}$ and normal deviations ($\mathbf{s}_\perp$), is illustrated. The two exponential decay functions $e^{-z/\sqrt{2D_0\tau_{ex}}}$ and $e^{-z/\sqrt{D_0\tau_{sf}}}$, describing respectively the spatial distribution of $\mathbf{s}_\parallel$ and $\mathbf{s}_\perp$, are derived in the main text. $\mathbf{P}^z_{FE}$ indicates the ferroelectric polarization in the FE part of the interface.

screening spin density $\mathbf{s}$ can still penetrate into the FM system within the nanometer scale, resulting in spin rearrangement within a much larger characteristic length than inferred from electrostatic charge screening (a few atomic layers). So for us thin FM films are most favorable. C_i is determined by the following electric neutrality constraint:

$$\mathcal{P}_s = \int dz|\mathbf{s}_\parallel| + \int dz|\mathbf{s}_\perp|, \tag{9}$$

$$\eta = \int dz|\mathbf{s}_\parallel| \Big/ \int dz(|\mathbf{s}_\parallel| + |\mathbf{s}_\perp|), \tag{10}$$

where $\mathcal{P}_s$ is the surface electron density due to the electrostatic screening over λ_m, and η is the spin polarization of electron density in a FM within the Stoner mean-field theory [38]. We thus obtain

$$C_\parallel = \eta\mathcal{P}_s/\lambda_m, \quad C_\perp = (1-\eta)Q_m\mathcal{P}_s. \tag{11}$$

(a) For a half metal with $\eta = 1$, we have $C_\perp = 0$. The screening spins are fully polarized without any nonadiabatic deviation. (b) For a FM metal ($\eta < 1$), we expect changes of the magnetization on both the easy and hard axes, respectively given as (d is the FM film thickness)

$$\Delta\mathbf{M}_\parallel = \eta\frac{\mathcal{P}_s}{d}\mu_B, \quad \Delta\mathbf{M}_\perp = (1-\eta)\frac{\mathcal{P}_s}{d}\mu_B. \tag{12}$$

An outward/inward electric field acting on a FM interface (implying an effective positive/negative charge screening within the FM metal surface) suppresses/induces the surface magnetization, which is in line with first-principles results [19–21] and experimental observations [5,6,10,13]. Generally, noncollinear magnetic ordering in metals is well documented

experimentally (e.g., Ref. [39]), albeit it has a different origin than the one discussed here.

On the other hand, the established theory of FE driven by inhomogeneous magnetism [24–29] predicts an intrinsic coupling between spin, charge, and ionic displacement stabilizing ferroelectricity. Our scenario is different in that FE polarization (and electric field) stems actually from the FE surface which triggers the spin spiral in a FM. The latter carries a spin current with an associated Aharonov-Casher effect and/or Dzyaloshinkii-Moriya (DM) interaction [24,40]. In this sense we are looking here at ME coupling caused by an emergent inverse DM interaction at multiferroic interfaces. No symmetry-breaking atomic displacements in FM are expected, as in general the phonon-magnon coupling is quite weak (this may not be so for magnetoelastically coupled FMs; as shown below we predict ME-induced changes in the magnetic anisotropy that may lead to elastic dynamics in FMs through the respective intrinsic terms in the FM free-energy density). As discussed below FE polarization is also affected by ME coupling, which may result in ionic displacement at the FE interface via intrinsic piezoelectric coupling in the FE. Thus, the present mechanism interplays with or affects in general other ME couplings, but can still be distinguished via the distinctive symmetry and topology features of the spiral, leading, e.g., to the emergence of an interface spin-orbital interaction that shows up in the electric and thermoelectric transport properties of FE/FM tunnel structures [41].

III. LINEAR MAGNETOELECTRIC COUPLING

The surface charge density in the FM subsystem and the relaxed coarse-grained FE polarization $\mathbf{P}_0$ at the interface obey $e\mathcal{P}_s = P_0^z$. Considering the s-d exchange interaction H_{sd} we arrive at an effective interfacial ME interaction

$$E_{\rm ME} = \alpha_{\rm ME} P_0^z M_0 \quad \text{with} \quad \alpha_{\rm ME} = \frac{\eta J_{ex}}{edM_s}. \tag{13}$$

$\mathbf{M}_0$ is the coarse-grained magnetization closest to the interface.

Clearly, such a linear surface ME effect is pronounced in FM films with thickness in the range of λ_m. For Co/$BaTiO_3$ (BTO) heterostructures, $\lambda_m = 38 \pm 12$ nm [37], together with $J_{ex} \approx 0.1$ eV/atom, $\eta \approx 0.4$ [38], $M_s = 1.43\times10^6$ A/m [42], and Co film with thickness $d = 40$ nm, we arrive at $\alpha_{\rm ME} = 0.699$ s/F, which agrees reasonably with the experimental estimate of 0.27 s/F [42]. Note that the sign of the magnetoelectrically induced "interface anisotropy" energy density $E_{\rm ME}$ is controllable by applying an external electric field. Thus, an electrically induced reversal of the total magnetization is possible for thin FM films [43–45], as suggested in experiments on the multiferroic tunnel juncotion Co/Plumbum Zirconate Titanate/Lanthanum Strontium Manganite [13].

IV. MULTIFERROIC SURFACE

Let us inspect closely the profile of the spin-density wave. It possesses an exponential spiral in the rotating frame around $\hat{\mathbf{e}}_{M_\parallel}$ (see Fig. 1),

$$\begin{aligned}\tilde{\mathbf{M}}(\mathbf{r}) = {} & \mathbf{e}_{M_{\perp,x}} C_\perp e^{-\mathbf{Q}_m\cdot\mathbf{r}} \cos(\mathbf{Q}_m\cdot\mathbf{r}+\theta_0) \\ & + \mathbf{e}_{M_{\perp,y}} C_\perp e^{-\mathbf{Q}_m\cdot\mathbf{r}} \sin(\mathbf{Q}_m\cdot\mathbf{r}+\theta_0) \\ & + \mathbf{e}_{M_\parallel}(M_s + C_\parallel e^{-z/\lambda_m}).\end{aligned} \tag{14}$$

Following the arguments of Refs. [25,27] we may conclude from Eq. (14) that the associated charge distribution profile is

$$\mathbf{P}_{\rm FM}(\mathbf{r}_{\rm FM}) = -\gamma\chi_e\nabla(\tilde{\mathbf{M}}^2) + \gamma'\chi_e[(\tilde{\mathbf{M}}\cdot\nabla)\tilde{\mathbf{M}} - \tilde{\mathbf{M}}(\nabla\cdot\tilde{\mathbf{M}})], \tag{15}$$

where χ_e is the dielectric susceptibility, and γ and γ' are the ME coupling constants. The first term on the right-hand side (RHS) in Eq. (15) is important for spatially and amplitude-modulated magnetic order, such as for YMn_2O_5 [46]. To leading order it results in magnetically driven effective polarization along $\mathbf{e}_z$ ($\mathbf{P}^z_{\rm FM} = -\frac{1}{V}\int d^3\mathbf{r}\gamma\chi_e\nabla(\tilde{\mathbf{M}}^2) \approx \frac{2C_\parallel M_s\gamma\chi_e}{d}\mathbf{e}_z$).

We refer to the second term in Eq. (15) to as the spin current or the inverse DM mechanism. It is crucial if the magnetization breaks the chiral symmetry as in $TbMnO_3$ [47], in which case the electric polarization is ascribed to a noncollinear spiral magnetic structure, $\mathbf{P} \sim \mathbf{e}_{M_\parallel}\times\mathbf{Q}_m$ [24,25,28]. For a surface magnetic order, depending on the orientation of the local undisturbed magnetization $\mathbf{M}$, we end up subsequently with a longitudinal or transverse conical spin-density wave.

It should be noted that for single-phase multiferroics only the transverse conical spins coincide with the ferroelectricity [48]. The situation is very different for a FM surface: Due to the breaking of spatial inversion symmetry of the induced exponentially decaying spin density, ME coupling is allowed regardless of the relative orientation between the spin spiral axis $\mathbf{e}_{M_\parallel}$ and the magnetic modulation vector $\mathbf{Q}_m$. We find two distinct cases:

(i) Normal $\mathbf{M}$ with an exponential longitudinal conical spin density ($\mathbf{e}_{M_\parallel} \parallel \mathbf{Q}_m$) gives rise to a proper-screw charge distribution, $\mathcal{P}^\perp_{\rm FM} = -\gamma'\chi_e M_s Q_m C_\perp e^{-Q_m z}[(\mathbf{e}_{M_{\perp,x}} - \mathbf{e}_{M_{\perp,y}})\cos(Q_m z+\theta_0) + (\mathbf{e}_{M_{\perp,x}} + \mathbf{e}_{M_{\perp,y}})\sin(Q_m z+\theta_0)]$. By integrating over the film thickness we infer for the in-plane, averaged screening distribution

$$\mathbf{P}^\perp_{\rm FM} = \frac{1}{V}\int d\mathbf{r}\mathcal{P}^{\rm FM}_\perp = \frac{C_\perp M_s\gamma'\chi_e}{d}\mathbf{e}'_{M_\perp}, \tag{16}$$

with $\mathbf{e}'_{M_\perp} = (\mathbf{e}_{M_{\perp,x}}\cos\theta_0 - \mathbf{e}_{M_{\perp,y}}\sin\theta_0)$. It is obvious that $\mathbf{P}^\perp_{\rm FM}$ does depend linearly on the magnetization $\mathbf{M}$ and/or an applied gate bias through $C_\perp$.

(ii) For in-plane $\mathbf{M}$ with an exponential transverse conical spin density ($\mathbf{e}_{M_\parallel} \perp \mathbf{Q}_m$) we infer

$$\mathbf{P}^\parallel_{\rm FM} = \frac{C_\perp^2\gamma'\chi_e}{2d}(\mathbf{e}_{M_\parallel}\times\mathbf{Q}_m) + \frac{C_\perp M_s\gamma'\chi_e}{d}\mathbf{e}_{M_\parallel}. \tag{17}$$

The first part is finite if the chiral symmetry is broken and delivers a second-order contribution to the surface charge distribution, as compared to the second term that results from the magnetic amplitude modulation.

To estimate semiquantitatively the interfacial multiferrocity, let us consider a Co/BTO multilayer as a representative composite heterostructure for which we have a single out-of-interface FE polarization $\mathbf{P}_{\rm FE} = 0.27$ C/m^2 in BTO at room temperature [49]. Q_m is the most important parameter here and might be strongly affected by the interface effects. The surface modifications however are difficult to measure. In the estimation we take the bulk value of the Co film, $1/|Q_m| = 4.7$ nm [1]. $\chi_e \approx 1$ and the other parameters η

and M_s in Co are the same as in the evaluation of the interfacial ME interaction above. The ME coupling constant γ' (and γ) is calculated by taking the spin-driven ferroelectricity $|P_c| = |\gamma' \chi_e m_b m_c Q_m| = 500\ \mu\text{C/m}^2$ in $TbMnO_3$ with the spiral spins $\mathbf{M}_i = \mathbf{m}_b \cos(\mathbf{Q}_m \cdot \mathbf{r}_i) + \mathbf{m}_c \sin(\mathbf{Q}_m \cdot \mathbf{R}_i)$, in which $\mathbf{m}_b = [0,3.9,0]\mu_B$, $\mathbf{m}_c = [0,0,2.8]\mu_B$, and $\mathbf{Q}_m = [0,0.27,0]$ [50]. With these values, we characterize the surface charge redistribution ina FM as

$$\left|\mathbf{P}^z_{\text{FM}}\right| = 2C_{\parallel} Q_m M_s \gamma \chi_e = 0.54\ \mu\text{C/m}^2, \tag{18}$$

$$|\mathbf{P}^{\perp}_{\text{FM}}| \approx |\mathbf{P}^{\parallel}_{\text{FM}}| = C_{\perp} Q_m M_s \gamma' \chi_e = 0.40\ \mu\text{C/m}^2, \tag{19}$$

which is comparable with the FE polarization in the single-phase multiferroic $LiCu_2O_2$ [51].

V. POLARIZATION DYNAMICS

For a FM/FE interface the ME coupling drives in turn the polarization profile in the FE part and may thus trigger the lattice dynamics. Phenomenologically, this effect is readily clear: the FE free-energy density attains the additional contribution E_{ME} facilitating thus energy exchange with the FM system. Thus, the energy for building up the spiral in the FM part is supplied partly by the FE system which affects the FE or elastic order near the interface. Such dynamical effects are directly captured by the scheme of Refs. [43–45]. It is noteworthy that the direction of $\mathbf{P}_{\text{FM}}$ is controllable by the magnetization $\mathbf{M}$. As a consequence, for thin FE films on a FM substrate such as ultrathin $BaTiO_3$ films grown on Fe(001) as reported in Ref. [52], the FE polarization is in principle magnetically susceptible [44].

VI. INTERFACE MAGNETOELECTRIC ANISOTROPY

The multiferroic surface effect exposed here is intrinsic and general, even though the details and its relevance are material and system dependent as discussed above. The magnetic dependence of the (nonvolatile) FE polarization causes a nonvolatile $\mathbf{P}_{\text{FM}}$ in a FM. This has important implications for data storage technology in view of the nonvolatile multiferroic memory. As far as the magnetoelectric transport in a FM film is concerned, we note that $\mathbf{P}_{\text{FM}}$ is linearly determined by the normal FE polarization $P^z_0(E)$ through Eq. (11) with the surface electron density being $e\mathcal{P}_s = P^z_0(E)$ and under the constraint of electrical neutrality. Upon a sudden turn-off the normal FE polarization $P^z_0(E)$ induces simultaneously a large charge current $\sim d\mathbf{P}_{\text{FM}}/dt$ in FM which results in marked changes of the charge resistivity of the FM subsystem. This conclusion of our model offers an explanation of the experimental observation for Fe_3O_4/Plumbum Magnesium Niobate-Plumbum Titanate (PMN-PT)[001] heterostructures [53], where sharp peaks in $|\frac{d\ln R}{dE}|$ for Fe_3O_4 were observed as the FE polarization vector in PMN-PT was electrically switched by an external electric field E from out of plane to in plane near the coercive field even at room temperature, far away from the Verwey metal-insulator transition temperature around 125 K.

Another interesting aspect of multiferroic surface effects concerns the perpendicular magnetic anisotropy energy of the FM film [5],

$$F^{\perp}_{\text{FM}} = \left(-\frac{1}{2}\mu_0 \tilde{M}_s^2 + K_u\right) + \frac{K_s}{d}, \tag{20}$$

where μ_0 is the permeability of free space, K_u is the uniaxial crystalline anisotropy, and K_s is the surface anisotropy. $\tilde{M}_s$ is the saturation magnetization which can be modified by surface charges [54]. According to Eqs. (12) the change of the anisotropy energy is expressed explicitly to a leading term as

$$\Delta K_s = -\frac{\tilde{\eta} M_s \mathcal{P}_s}{d} \tag{21}$$

with $\tilde{\eta} = \mu_0 \mu_B \eta/2$. For M_s and K_u constant under the bias voltage application, ΔK_s acts as an additional effect of the surface anisotropy, linearly induced by the external electric field, which is also in line with the experimental observations [5–8] as well as the first-principles studies [16–21]. Note that $\Delta K_s d$ is not constant across the whole thickness range because of the less efficient surface screening in the spin channel over the nanometer scale; it shows thickness dependence in thin FM films within the magnetic screening length λ_m. Such a dependence characterizes the spin-penetration length λ_m which is larger than the modified Thomas-Fermi length (of the order of angstroms) in FM metals [32], and may play a role in the constant deviation of $\Delta K_s d$ in the experiment on Co/P(VDF-TrFE) [10]. A further important consequence is the fictitious spin electric field and the effective spin-orbit coupling associated with magnetic textures [35] which may be exploited for interface-limited spintronic applications.

VII. CONCLUSIONS

We unraveled the possibility of the existence of an exponential spiral spin texture that develops at a FM interface due to an interplay of spin-dependent charge accumulation, the *s-d* exchange interaction, spin diffusion, and electrostatic interactions. The noncollinearity of interfacial spin order in a FM gives rise to an intrinsic multiferrocity in the corresponding region, rendering thus a ME coupling. Due to the large spin-diffusion length in FM metals, ME effects may have substantial influence on FM layers with thickness over tens of nanometers. The predicted phenomena bear a genuine potential for applications, e.g., to nonvolatile multiferroic memory devices with heterogeneous read/write capability through the interfacial ME coupling.

ACKNOWLEDGMENTS

This work was supported by the National Basic Research Program of China (No. 2012CB933101), the German Research Foundation (No. SFB 762, and BE 2161/5-1), the National Natural Science Foundation of China (No. 11104123), the Program for Changjiang Scholars and Innovative Research Team in University (No. IRT1251), and the Fundamental Research Funds for the Central Universities (No. 2022013zrct01/2022013zr0017).

[1] C. A. F. Vaz, J. A. C. Bland, and G. Lauhoff, Rep. Prog. Phys. **71**, 056501 (2008).

[2] J. Mannhart, D. Blank, H. Y. Hwang, and A. J. Millis, MRS Bull. **33**, 1027 (2008).

[3] C. A. F. Vaz, J. Hoffman, C. H. Ahn, and R. Ramesh, Adv. Mater. **22**, 2900 (2010).

[4] J. P. Velev, S. S. Jaswal, and E. Y. Tsymbal, Phil. Trans. R. Soc. A **369**, 3069 (2011).

[5] T. Maruyama, Y. Shiota, T. Nozaki, K. Ohta, N. Toda, M. Mizuguchi, A. A. Tulapurkar, T. Shinjo, M. Shiraishi, S. Mizukami, Y. Ando, and Y. Suzuki, Nature Nanotech. **4**, 158 (2009).

[6] T. Nozaki, Y. Shiota, M. Shiraishi, T. Shinjo, and Y. Suzuki, Appl. Phys. Lett. **96**, 022506 (2010).

[7] T. Nozaki, Y. Shiota, S. Miwa, S. Murakami, F. Bonell, S. Ishibashi, H. Kubota, K. Yakushiji, T. Saruya, A. Fukushima, S. Yuasa, T. Shinjo, and Y. Suzuki, Nature Physics **8**, 491 (2012).

[8] Y. Shiota, F. Bonell, S. Miwa, N. Mizuochi, T. Shinjo, and Y. Suzuki, Appl. Phys. Lett. **103**, 082410 (2013).

[9] H. J. A. Molegraaf, J. Hoffman, C. A. F. Vaz, S. Gariglio, D. van der Marel, C. H. Ahn, and J.-M. Triscone, Adv. Mater. **21**, 3470 (2009).

[10] A. Mardana, S. Ducharme, and S. Adenwalla, Nano Lett. **11**, 3862 (2011).

[11] T. Nozaki, Y. Shiota, S. Miwa, S. Murakami, F. Bonell, S. Ishibashi, H. Kubota, K. Yakushiji, T. Saruya, A. Fukushima, S. Yuasa, T. Shinjo, and Y. Suzuki, Nature Physics **8**, 491 (2012).

[12] S. Valencia, A. Crassous, L. Bocher, V. Garcia, X. Moya, R. O. Cherifi, C. Deranlot, K. Bouzehouane, S. Fusil, A. Zobelli, A. Gloter, N. D. Mathur, A. Gaupp, R. Abrudan, F. Radu, A. Barthélémy, and M. Bibes, Nature Materials **10**, 753 (2011).

[13] D. Pantel, S. Goetze, D. Hesse, and M. Alexe, Nature Materials **11**, 289 (2012).

[14] C.-G. Duan, S. S. Jaswal, and E. Y. Tsymbal, Phys. Rev. Lett. **97**, 047201 (2006).

[15] M. Fechner, I. V. Maznichenko, S. Ostanin, A. Ernst, J. Henk, P. Bruno, and I. Mertig, Phys. Rev. B **78**, 212406 (2008).

[16] K. Nakamura, R. Shimabukuro, Y. Fujiwara, T. Akiyama, T. Ito, and A. J. Freeman, Phys. Rev. Lett. **102**, 187201 (2009).

[17] M. Tsujikawa and T. Oda, Phys. Rev. Lett. **102**, 247203 (2009).

[18] H. X. Yang, M. Chshiev, B. Dieny, J. H. Lee, A. Manchon, and K. H. Shin, Phys. Rev. B **84**, 054401 (2011).

[19] C.-G. Duan, J. P. Velev, R. F. Sabirianov, Z. Zhu, J. Chu, S. S. Jaswal, and E. Y. Tsymbal, Phys. Rev. Lett. **101**, 137201 (2008).

[20] J. M. Rondinelli, M. Stengel, and N. A. Spaldin, Nature Nanotech. **3**, 46 (2008).

[21] T. Cai, S. Ju, J. Lee, N. Sai, A. A. Demkov, Q. Niu, Z. Li, J. Shi, and E. Wang, Phys. Rev. B **80**, 140415(R) (2009).

[22] J. D. Burton and E. Y. Tsymbal, Phil. Trans. R. Soc. A **370**, 4840 (2012), and references therein.

[23] C. A. F. Vaz, J. Phys.: Condens. Matter **24**, 333201 (2012), and references therein.

[24] H. Katsura, N. Nagaosa, and A. V. Balatsky, Phys. Rev. Lett. **95**, 057205 (2005).

[25] M. Mostovoy, Phys. Rev. Lett. **96**, 067601 (2006).

[26] I. A. Sergienko, C. Sen, and E. Dagotto, Phys. Rev. Lett. **97**, 227204 (2006).

[27] J. J. Betouras, G. Giovannetti, and J. van den Brink, Phys. Rev. Lett. **98**, 257602 (2007).

[28] C. L. Jia, S. Onoda, N. Nagaosa, and J. H. Han, Phys. Rev. B **76**, 144424 (2007).

[29] H. J. Xiang, E. J. Kan, Y. Zhang, M.-H. Whangbo, and X. G. Gong, Phys. Rev. Lett. **107**, 157202 (2011).

[30] M. Endo, S. Kanai, S. Ikeda, F. Matsukura, and H. Ohno, Appl. Phys. Lett. **96**, 212503 (2010).

[31] T. Seki, M. Kohda, J. Nitta, and K. Takanashi, Appl. Phys. Lett. **98**, 212505 (2011).

[32] S. Zhang, Phys. Rev. Lett. **83**, 640 (1999).

[33] M. Pajda, J. Kudrnovský, I. Turek, V. Drchal, and P. Bruno, Phys. Rev. B **64**, 174402 (2001).

[34] T. Moriya*Spin Fluctuations in Itinerant Electron Magnetism*, (Springer-Verlag, Berlin, Heidelberg, 1985); A. I. Liechtenstein *et al.*, J. Magn. Magn. Mater. **67**, 65 (1987); V. P. Antropov *et al.*, *ibid.* **200**, 148 (1999); A. Oswald *et al.*, J. Phys. F **15**, 193 (1985).

[35] G. Tatara, H. Kohno, and J. Shibata, Phys. Rep. **468**, 213 (2008).

[36] S. Zhang and Z. Li, Phys. Rev. Lett. **93**, 127204 (2004).

[37] J. Bass and W. P. Pratt Jr., J. Phys.: Condens. Matter **19**, 183201 (2007).

[38] R. J. Soulen, J. M. Byers, M. S. Osofsky, B. Nadgorny, T. Ambrose, S. F. Cheng, P. R. Broussard, C. T. Tanaka, J. Nowak, J. S. Moodera, A. Barry, and J. Coey, Science **282**, 85 (1998).

[39] C. Pfleiderer, S. R. Julian, and G. G. Lonzarich, Nature (London) **414**, 427 (2001); N. Doiron-Leyraud *et al.*, *ibid.* **425**, 595 (2003); C. Pfleiderer *et al.*, *ibid.* **427**, 227 (2004); M. Uchida *et al.*, Science **311**, 359 (2006); M. Uchida, N. Nagaosa, J. P. He, Y. Kaneko, S. Iguchi, Y. Matsui, and Y. Tokura, Phys. Rev. B **77**, 184402 (2008); S. Meckler, N. Mikuszeit, A. Preßler, E. Y. Vedmedenko, O. Pietzsch, and R. Wiesendanger, Phys. Rev. Lett. **103**, 157201 (2009); P. Ferriani, K. von Bergmann, E. Y. Vedmedenko, S. Heinze, M. Bode, M. Heide, G. Bihlmayer, S. Blügel, and R. Wiesendanger, *ibid.* **101**, 027201 (2008); M. Bode *et al.*, Nature (London) **447**, 190 (2007).

[40] F. Meier and D. Loss, Phys. Rev. Lett. **90**, 167204 (2003).

[41] C. L. Jia and J. Berakdar, Appl. Phys. Lett. **98**, 042110 (2011); App. Phys. Lett. **98**, 192111 (2011); Y. Wang *et al.*, *ibid.* **103**, 052903 (2013); C. L. Jia and J. Berakdar, Phys. Rev. B **81**, 052406 (2010).

[42] N. Jedrecy, H. J. von Bardeleben, V. Badjeck, D. Demaille, D. Stanescu, H. Magnan, and A. Barbier, Phys. Rev. B **88**, 121409 (2013).

[43] A. Sukhov, C. Jia, P. P. Horley, and J. Berakdar, J. Phys.: Condens. Matter **22**, 352201 (2010).

[44] C. Jia, A. Sukhov, P. P. Horley, and J. Berakdar, J. Phys.: Conf. Ser. **303**, 012061 (2011).

[45] P. P. Horley, A. Sukhov, C. Jia, E. Martinez, and J. Berakdar, Phys. Rev. B **85**, 054401 (2012).

[46] N. Hur, S. Park, P. A. Sharma, J. Ahn, S. Guha, and S.-W. Cheong, Nature (London) **429**, 392 (2004).

[47] Y. Tokura and S. Seki, Adv. Mater. **22**, 1554 (2010).

[48] T. Kimura, Annu. Rev. Condens. Matter Phys. **3**, 93 (2012).

[49] K. Rabe, Ch. H. Ahn, and J.-M. Triscone, eds., *Physics of Ferroelectrics: A Modern Perpective* (Springer, Berlin, 2007).

[50] Y. Yamasaki, H. Sagayama, T. Goto, M. Matsuura, K. Hirota, T. Arima, and Y. Tokura, Phys. Rev. Lett. **98**, 147204 (2007).

[51] S. Seki, Y. Yamasaki, M. Soda, M. Matsuura, K. Hirota, and Y. Tokura, Phys. Rev. Lett. **100**, 127201 (2008).

[52] H. L. Meyerheim, F. Klimenta, A. Ernst, K. Mohseni, S. Ostanin, M. Fechner, S. Parihar, I. V. Maznichenko, I. Mertig, and J. Kirschner, Phys. Rev. Lett. **106**, 087203 (2011).

[53] M. Liu, J. Hoffman, J. Wang, J. Zhang, B. Nelson-Cheeseman, and A. Bhattacharya, Sci. Rep. 3 (2013).

[54] S. J. Gong, C.-G. Duan, Z.-Q. Zhu, and J.-H. Chu, Appl. Phys. Lett. **100**, 122410 (2012).